

# 1 **A monthly tidal envelope classification for semidiurnal regimes in** 2 **terms of the relative proportions of the S<sub>2</sub>, N<sub>2</sub>, and M<sub>2</sub> constituents**

3 Do-Seong Byun<sup>1</sup>, Deirdre E. Hart<sup>2</sup>

4 <sup>1</sup>Ocean Research Division, Korea Hydrographic and Oceanographic Agency, Busan 49111, Republic of Korea

5 <sup>2</sup>School of Earth and Environment, University of Canterbury, Christchurch 8140, Aotearoa New Zealand

6 *Correspondence to:* Deirdre E. Hart (deirdre.hart@canterbury.ac.nz)

7 **Abstract.** Daily tidal water level variations are a key control on shore ecology; on access to marine environments via ports,  
8 jetties and wharves; on drainage links between the ocean and coastal hydrosystems such as lagoons and estuaries; and on the  
9 duration and frequency of opportunities to access the intertidal zone for recreation and food harvesting purposes. Further, high  
10 perigean-spring tides interact with extreme weather events to produce significant coastal inundation in low-lying coastal  
11 settlements such as on deltas. Thus an understanding of daily through to monthly tidal envelope characteristics is fundamental  
12 to resilient coastal management and development practices. For decades, scientists have described and compared daily tidal  
13 forms around the world's coasts based on the four main tidal amplitudes. Our paper builds on this 'daily' method by adjusting  
14 the constituent analysis to distinguish the different monthly types of tidal envelope occurring in the semidiurnal coastal waters  
15 around New Zealand. Analyses of tidal records from 27 stations are used alongside data from the FES2014 tide model in order  
16 to find the key characteristics and constituent ratios of tides that can be used to classify monthly tidal envelopes. The resulting  
17 monthly tidal envelope classification approach described (*E*) is simple, complementary to the successful and much used daily  
18 tidal form factor (*F*), and of use for coastal flooding and maritime operation management and planning applications, in areas  
19 with semidiurnal regimes.

20 **Copyright statement (will be included by Copernicus)**

## 21 **1 Introduction**

22 Successful human-coast interactions in the world's low-lying areas are predicated upon understanding the temporal and spatial  
23 variability of sea levels (Nicholls et al., 2007; Woodworth et al., 2019). This is particularly the case in island nations like New  
24 Zealand (NZ), where over 70% of the population reside in coastal settlements (Stephens, 2015). An understanding of tidal  
25 water level variations is fundamental to resilient inundation management and coastal development practices in such places, as  
26 well as to accurately resolving non-tidal signals of global interest such as in studies of sea level change (Cartwright, 1999;  
27 Masselink et al., 2014; Olson, 2012; Pugh, 1996, Stammer et al., 2014).

28 In terms of daily cycles, tidal form factors or form numbers ( $F$ ) based on the amplitudes of the four main tidal constituents  
29 ( $K_1$ ,  $O_1$ ,  $M_2$ ,  $S_2$ ) have been successfully used to classify tidal observations from the world's coasts into four types of tidal  
30 regime for nearly a century (Fig. 1a). Originally developed by van der Stok (1897) based on three regime types, with a fourth  
31 type added by Courtier (1938), this simple and useful daily form factor comprises a ratio between diurnal and semidiurnal tide  
32 amplitudes via the equation:

33 
$$F = \frac{K_1 + O_1}{M_2 + S_2} \quad (1)$$

34 The results classify tides into those which roughly experience one high and one low tide per day (diurnal regimes); or two  
35 approximately equivalent high and low tides per day (semidiurnal regimes); or two unequal high and low tides per day (mixed  
36 semidiurnal dominant or mixed diurnal dominant regimes) (e.g. Defant 1958).

37 Albeit not part of their original design, some interpretation of the tidal envelope types observed at fortnightly and monthly  
38 timescales has accompanied use of daily tidal form classifications (e.g. Pugh, 1996; Pugh & Woodworth, 2014). The daily  
39 tidal form factor identifies the typical number (1 or 2) and form (equal or unequal tidal ranges) of tidal cycles within a lunar  
40 day (i.e. 24 hours and 48 minutes) at a particular site. In contrast, the term 'tidal envelope' describes a smooth curve outlining  
41 the extremes (maxima and minima) of the oscillating daily tidal cycles occurring at a particular site through a specified time  
42 period. The envelope time period of interest in this paper is monthly.

43 Tidal envelopes at monthly scales depend on tidal regime. In general, semidiurnal tidal regimes often feature two spring-neap  
44 tidal cycles per synodic (lunar) month. These two spring-neap tidal cycles are usually of unequal magnitude, due to the effect  
45 of the moon's perigee and apogee, which cycle over the period of the anomalistic month. In contrast, diurnal tidal regimes  
46 exhibit two pseudo spring-neap tides per sidereal month. For semidiurnal regions where the  $N_2$  constituent contributes  
47 significantly to tidal ranges, tidal envelope classification should consider relationships between the  $M_2$ ,  $S_2$ , and  $N_2$  amplitudes.

48 The waters around NZ represent one such region: here the daily tidal form is consistently semidiurnal, but large differences  
49 occur between sites within this region in terms of their typical tidal envelope types over fortnightly to monthly timescales.

50 More than eighty years after the development of the ever-useful daily tidal form factors, attention to the regional distinction  
51 between different tidal envelope types within the semidiurnal category forms the motivation for this paper. In this first explicit  
52 attempt to classify monthly tidal envelope types, we examined the waters around NZ, a strong semidiurnal regime with  
53 relatively weak diurnal tides (daily form factor  $F < 0.15$ ) and variation in the importance of the  $S_2$  and  $N_2$  amplitude ratios.

54 The result is an approach for classifying monthly tidal envelope types that is transferable to any semidiurnal regime. As well  
55 as providing greater understanding of the tidal regimes of NZ, we hope that our paper opens the door for new international  
56 interest in classifying tidal envelope variability at multiple timescales, work which would have direct coastal and maritime  
57 management application including contributing to explanations of the processes behind delta city coastal flooding hazards and  
58 their regional spatial variability.

59 **2 Methodology**

60 **2.1 Study area**

61 New Zealand (Fig. 2) is a long (1600 km), narrow ( $\leq 400$  km) country situated in the south-western Pacific Ocean and straddling  
62 the boundary between the Indo-Australian and Pacific plates. Its three main islands, the North Island, the South Island, and  
63 Stewart Island/ Rakiura, span a latitudinal range from about  $34^{\circ}$  to  $47^{\circ}$  South. The tidal regimes in the surrounding coastal  
64 waters are semidiurnal, with variable diurnal inequalities, and feature micro through to macro tidal ranges. Classic spring-neap  
65 cycles are present in western areas of NZ, while eastern areas feature distinct perigean-apogean influences (Byun and Hart,  
66 2015; Heath, 1977, 1985; LINZ, 2017b; Walters et al., 2001).

67 Highly complex tidal propagation patterns occur around NZ, including a complete semidiurnal tide rotation, with tides  
68 generally circulating around the country in an anticlockwise direction. This occurs due to the forcing of  $M_2$  and  $N_2$  tides by  
69 their respective amphidromes, situated northwest and southeast of the country respectively, producing trapped Kelvin waves  
70 (for a map of the  $K_1$  and  $M_2$  amphidromes see Fig. 5.1 in Pugh and Woodworth, 2014). The  $S_2$  and  $K_1$  tides propagate northeast  
71 to southwest around NZ. This results in a southward travelling Kelvin wave along the west coast, and small  $S_2$  and  $K_1$   
72 amplitudes along the east coast, with amphidromes occurring southeast of NZ (Walters et al. 2001; 2010). Around Cook Strait,  
73 the waterway between the two main islands, tides travelling north along the east coast run parallel to tides travelling south  
74 along the west coast. The pronounced differences between these east/west tidal states, combined with their tidal range  
75 differences, together produce marked differences in amplitude and strong current flows through the strait (Heath, 1985; Walters  
76 et al., 2001, 2010).

77 **2.2 Data analysis approach**

78 Year-long sea level records were sourced from a total of 27 stations spread around NZ (Fig. 2): eighteen 1 minute-interval  
79 records from Land Information New Zealand (LINZ, 2017a); and nine 1 hour-interval records from the National Institute of  
80 Water and Atmospheric Research (NIWA, 2017). For both the LINZ and NIWA data, an individual year of good quality hourly  
81 data was selected for analysis per site from amongst the multi-year records. The 27 individual year sea level records were then  
82 harmonically analysed using T\_Tide (Pawlowicz et al., 2002) with the nodal (satellite) modulation correction option, to  
83 examine spatial variation in the main tidal constituents' amplitudes, phase lags, and amplitude ratios between regions (see  
84 Table A1 for raw results) and to compare them with values obtained from the tidal potential or Equilibrium Tide. An additional  
85 set of tidal constituent amplitudes was obtained from Tables 1 and 3 of Walters et al. (2010), derived from 33 records of  
86 between 14 and 1900 days in length, from around the greater Cook Strait area, where spring-neap tides are the strongest in the  
87 country.

88 We then classified the monthly tidal envelope types found around NZ based on examination of constituent ratios produced  
89 from the tidal harmonic analysis results, data from the FES2014 tide model (see Carrère et al., 2016 for a full description of  
90 this model), and examination of tidal envelope plots. Due to the strong semidiurnal tidal regimes in the study area, and similar

91 to the approach of Walters et al. (2010), we were able to ignore diurnal ( $K_1$ ,  $O_1$ ) effects and simply consider the effects of  
92 spring-neap ( $M_2$ ,  $S_2$ ) and perigean-apogean cycles ( $M_2$ ,  $N_2$ ) in our monthly tidal envelope type characterisation.

93 **3 Results**

94 **3.1 Key tidal constituent amplitudes and amplitude ratios**

95 In order to better understand the key constituents responsible for shaping tidal height forms around NZ, we first mapped spatial  
96 variability in the amplitudes of the  $M_2$ ,  $S_2$ ,  $N_2$   $K_1$ , and  $O_1$  constituents and  $F$  (Fig. 3), and in the ratio values of the semidiurnal  
97 constituent amplitudes (Fig. 4). Table 1 summarises these data, and contrasts them with those from Equilibrium Theory (values  
98 obtained from Defant, 1958), while Table A1 catalogues the detailed results.

99 Tidal amplitude ratio comparisons confirmed that the waters around NZ are dominated by the three astronomical semidiurnal  
100 tides:  $M_2$ ,  $S_2$  and  $N_2$  (Table 1), the combination of which can generate fortnightly spring-neap tides ( $M_2$  and  $S_2$ ) and monthly  
101 perigean-apogean tides ( $M_2$  and  $N_2$ ). Figure 3 shows the relatively minor magnitudes of diurnal constituent amplitudes ( $O_1$ ,  
102  $K_1$ ), as well as revealing the stronger west coast amplitudes of the spring-neap cycle generating constituents ( $M_2$  and  $S_2$ ), the  
103 relatively weak  $S_2$  amplitudes overall (half that of Equilibrium Theory), and the more concentric pattern around NZ of the  
104 perigean-apogean cycle generating  $N_2$  amplitude (Fig. 3c).

105 In terms of the semidiurnal constituent amplitude ratios, Fig. 4 and Table 1 show that  $\frac{S_2}{M_2}$  values cover a broad range around  
106 NZ (0.04 to 0.47), with most sites exhibiting smaller values (<0.3 at 26 out of 27 sites) than that of Equilibrium Theory (0.47).

107 In contrast,  $\frac{N_2}{M_2}$  amplitude ratios were found to be more stable around NZ (values ranging from 0.16 to 0.23) and similar in  
108 magnitude to Equilibrium Theory (i.e. 0.19). By grouping the constituent amplitude and amplitude ratio results (Fig. 3 to 4),  
109 we were able to differentiate four distinct monthly tidal envelope regimes around NZ (Table 1), with Types 1 and 4  
110 distinguished as follows:

111 • Firstly, ‘*spring-neap*’ type tidal regimes (Type 1) occur where the  $S_2$  tide amplitude is large compared to that of the  
112  $N_2$  (Table 1, Fig. 3). In these areas there are two spring-neap tides per month with similar ranges, and negligible  
113 influence of perigean-apogean cycles. Type 1 regimes occur on the Kapiti and Cook Strait area (Fig. 2), where the  
114  $N_2$  and  $M_2$  amplitudes reduce by 75 to 90%, but the  $S_2$  amplitude reduces by only about 30%, compared to on the  
115 western coasts both north and south of this central NZ area.

116 • In direct contrast, there are ‘*perigean-apogean*’ type tidal regimes (Type 4), in areas where the  $N_2$  amplitude strongly  
117 dominates over the  $S_2$  (Table 1, Fig. 3). In Type 4 regimes the  $M_2$  and the  $N_2$  tides combine to produce strong signals  
118 over monthly timeframes (27.6 days). Hence the highest tidal ranges in any given month occur in relation to the  
119 perigee, when the moon’s orbit brings it close to Earth, rather than in line with the moon’s phase, as is typical in

121 spring-neap regimes. Type 4 regimes occur, for example, around the northern Chatham Rise near Kaikoura, and as  
122 far north as Castlepoint on the east coast of the North Island.

123 The remaining coastal waters around NZ can be separated into two tidal sub-regions, one with strong spring-neap signals (Type  
124 2) and the other with strong perigean-apogean signals (Type 3), but both with overall mixed or *intermediate* monthly tidal  
125 envelope types (Table 1). We distinguished these two envelope types via the tides generated by variability in the amplitude  
126 ratios of  $\frac{S_2}{M_2}$  and  $\frac{N_2}{M_2}$  (i.e. of the spring-neap cycle, and perigean-apogean cycle, forming tides, respectively). In brief, the  $\frac{S_2}{M_2}$   
127 amplitude ratio varies widely around NZ, with highest values in the west, lowest values in the east, and intermediate values to  
128 the north and south, while variation in the  $\frac{N_2}{S_2}$  amplitude ratio exhibits an opposite pattern (compare Fig. 4a to 4c). By  
129 comparison, the  $\frac{N_2}{M_2}$  amplitude ratios are relatively stable and high, except in a relatively small area of Cook Strait to the Kapiti  
130 coast, where this ratio drops and thus spring-neap cycles predominate (see ‘spring-neap’ Type 1 regimes above). The variability  
131 in these two ratios means that, except where we find ‘spring-neap’ or ‘perigean-apogean’ monthly tidal envelope types, spring-  
132 neap tides do occur but the overall monthly envelope shape is fundamentally altered (asymmetrically) due to the perigean-  
133 apogean influence.

134

- 135 • In the first of the ‘intermediate’ sub-regions, tides exhibit two dominant, but unequal, spring-neap cycles per month  
136 due to subordinate perigean-apogean effects. We term this type of monthly tidal envelope an ‘*intermediate,*  
137 *predominantly spring-neap*’ type regime (Type 2). Here values of the  $\frac{N_2}{S_2}$  amplitude ratio are  $<1$ , with  $S_2$  amplitudes  
138 being only around 24 to 30% those of the  $M_2$  constituent (Fig. 3 and 4, Table 1). Also in these areas, values of the  
139  $\frac{S_2+N_2}{M_2}$  amplitude ratio are  $\geq 0.45$ . Type 2 tides occur, for example, at Westport and Puysegur.

140

- 141 • In the other ‘intermediate’ sub-region, tides exhibit a mainly perigean-apogean form with a weaker, but noticeable,  
142 spring-neap signal: we term this envelope type as ‘*intermediate, predominantly perigean-apogean*’ (Type 3). Here  
143 values of the  $\frac{N_2}{S_2}$  amplitude ratio are between 1.07 and 3.5, while values of the  $\frac{S_2+N_2}{M_2}$  amplitude ratio are between 0.28  
144 and 0.43 (Fig. 3 and 4, Table 1). Type 3 tides occur, for example, at Auckland and Sumner.

145 Figure 5 illustrates the four types of monthly tidal envelope found around NZ as idealised types, two with stronger spring-neap  
146 signals (Types 1 and 2, see Fig. 5 a-b) and two with stronger perigean-apogean signals (Types 3 and 4, see Fig. 5 c-d) while  
147 Fig. 2 includes a colour coded classification of the observation stations into the four tidal envelope types.

148 **3.2 A monthly tidal envelope factor ( $E$ ) for semidiurnal regimes**

149 The four types of monthly tidal envelope found around NZ are essentially different combinations of spring-neap and perigean-  
 150 apogean signals. Thus, in a similar manner to van der Stok's (1897) method for calculating *daily* tidal form factors, a *monthly*  
 151 tidal envelope factor ( $E$ ) may be calculated for semidiurnal tidal regions, including that of NZ, according to:

152 
$$E = \frac{M_2 + N_2}{M_2 + S_2}, \quad (2)$$

153 where  $M_2$ ,  $N_2$  and  $S_2$  refer to the constituent amplitudes. This equation can be further expressed as:

154 
$$E = \frac{1 + \frac{S_2 - x}{M_2}}{1 + \frac{S_2}{M_2}}, \quad \text{with } x = \frac{N_2}{S_2} \quad (2a)$$

155 
$$E = \frac{1 + \frac{N_2}{M_2}}{1 + \frac{N_2 - y}{M_2}}, \quad \text{with } y = \frac{S_2}{N_2} \quad (2b)$$

156

157  $E$  takes into account the roles of the  $S_2$  and  $N_2$  tides in spring-neap and perigean-apogean cycles, while also factoring in the  
 158 strong  $M_2$  tide influence in both types of cycle.  $E$  may be used to classify the monthly tidal envelope types of any semidiurnal  
 159 region (i.e. where  $F < 0.25$ ) based on the analysis of constituent amplitudes and ratios from local data. The boundaries between  
 160 our different NZ monthly tidal envelope types were as follows:

- 161 •  $E < 0.8$  indicates a Type 1 'spring-neap' regime;
- 162 •  $E$  between 0.8 and 1.0 indicates a Type 2 'intermediate, predominantly spring-neap' regime (with the upper bound  
 163 also corresponding to an amplitude ratio of  $\frac{N_2}{S_2} < 1$  in semidiurnal regimes);
- 164 •  $E$  between 1.0 and 1.15 indicates a Type 3 'intermediate, predominantly perigean-apogean' regime (with the lower  
 165 bound also corresponding to an amplitude ratio of  $\frac{N_2}{S_2} > 1$  in semidiurnal regimes); and
- 166 •  $E > 1.5$  indicates a Type 4 'perigean-apogean' regime (with the lower bound also corresponding to an amplitude ratio  
 167 of  $\frac{N_2}{S_2} > 4$  in our NZ regimes).

168

169 Here we explain how we set boundaries between the different envelope types around NZ using case study data and as  
 170 summarised in Fig. 6. Firstly, in any semidiurnal tidal regime ( $F < 0.25$ ) anywhere in the world where the amplitude ratio  $\frac{N_2}{S_2} <$   
 171 1, spring-neap cycles will feature clearly in the tidal height records. Thus, the boundary separating Types 1 and 2 from Types  
 172 3 and 4 occurs at  $\frac{N_2}{S_2} = 1$ , when also  $E = 1$ . Type 1 and 2 areas of the NZ coast are characterised by relatively larger  $S_2$  amplitudes  
 173 (19-40 cm) than areas with stronger perigean-apogean influences (2-18 cm) (Table 1). Secondly, tidal regimes with stronger  
 174 spring-neap signals include places where spring-neap cycles occur as consecutive fortnightly cycles of similar magnitude  
 175 (Type 1 or 'spring-neap' type regimes), and places where spring-neap signals dominate but with noticeable variability in the  
 176 magnitudes of consecutive cycles due to subordinate perigean-apogean influences (Type 2 or 'intermediate, spring-neap'

177 regimes). In NZ the strongest spring-neap influence occurs in the Cook Strait to Kapiti area, where harmonic analysis revealed  
178 an amplitude ratio of  $\frac{N_2}{S_2} = 0.35$  and an  $E$  value of 0.79 (Table 1). Examining the shapes of tidal height plots showed that Kapiti  
179 had the only completely spring-neap dominated tidal envelope amongst the case study sites. Hence the boundary between Type  
180 1 versus 2 was set as  $E = 0.790$  for NZ, just greater than that of Kapiti and below the next strongest spring-neap influenced  
181 site, Nelson, where  $E = 0.902$  (Fig. 6). Lastly, to set a boundary between ‘perigean-apogean’ and ‘intermediate, perigean-  
182 apogean dominant’ regimes (i.e. Types 3 versus 4), we again examined tidal height plots to determine a boundary value of  $E$   
183 = 1.15, between the ‘intermediate, perigean-apogean dominated’ type regime of Napier ( $E = 1.147$ ) and the ‘perigean-apogean’  
184 type regime of Kaikoura ( $E = 1.162$ ) (Table A1; Fig. 6).

185 In summary, Fig. 7 illustrates the monthly tidal envelope values and types in the waters around NZ using  $E$ . The west coast is  
186 characterised by Type 2 monthly tidal envelopes, with two unequal spring-neap cycles per month. As mentioned above, Type  
187 1 monthly tidal envelopes, with their defined spring-neap tides, are only found in the western Cook Strait to Kapiti Coast area.  
188 The Cook Strait’s tides were explored in detail by Walters et al. (2010): our Fig. 6 includes a re-analysis of their data using the  
189  $E$  ratios. Note that the Cook Strait data includes 4 sites in the Type 1 category, as well as a number of Type 2 and Type 4 sites,  
190 and one Type 3 site, revealing this small Strait to be a concentrated area of monthly tidal envelope diversity. Extensive areas  
191 of Type 3 ‘intermediate, perigean-apogean dominated’ regimes are found along the northeast and southeast coasts of NZ, while  
192 the central eastern coasts show Type 4 ‘perigean-apogean’ tidal envelopes. As shown in Fig. 1c, such regimes are unusual  
193 internationally, also occurring in limited areas of the Cook Islands; northeast of the Pitcairn Islands; in Canada’s Hudson Bay;  
194 in Alaska’s Bristol Bay; offshore of the North Carolina to Virginia coast in the United States of America; on the north coast of  
195 the Bahamas; and in the Gulf of Ob in Russia.

#### 196 **4 Discussion and conclusion**

197 The daily water level variations wrought by the tides are a key control on shore ecology and on the accessibility of marine  
198 environments via fixed port, jetty and wharf infrastructure. These variations also moderate the functioning of drainage links  
199 between the ocean and coastal hydrosystems; and determine the duration and frequency of opportunities to access the intertidal  
200 zone for recreation and food harvesting purposes. Fortnightly and monthly tidal envelope variations, such as those associated  
201 with spring-neap and perigean-apogean cycles, have similar moderating roles on human usage of intertidal and shoreline  
202 environments, and additionally these medium term variations in tide levels are important factors in coastal inundation risk  
203 (Menéndez & Woodworth, 2010; Stephens 2015; Stephens et al., 2014; Wood, 1978, 1986). High perigean-spring tides, for  
204 example, interact with extreme weather events (including low pressures, strong winds and extreme rainfall) to produce  
205 significant coastal inundation in low-lying coastal settlements such as in the ‘delta city’ of Christchurch (Hart et al., 2015).  
206 In a world of rising sea levels, and coastal inundation hazard cascades (Menéndez and Woodworth, 2010), having common  
207 ways of describing different types of tidal envelope is helpful for living safely and productively in coastal cities. This paper  
208 has employed observations from NZ and FES2014 model data to demonstrate a simple approach to classifying different

209 monthly tidal envelope types, applicable to semidiurnal regions anywhere. The result is a widely applicable monthly tidal  
210 envelope factor,  $E$ , for classifying semidiurnal regimes based on the amplitudes and amplitude ratios of three key constituents:  
211  $M_2$ ,  $S_2$ , and  $N_2$ .

212 At a very basic level, in any semidiurnal tidal regime anywhere in the world where the amplitude ratio of  $\frac{N_2}{S_2} < 1$ , then spring-  
213 neap cycles will be clearly visible in tidal height records, either as consecutive fortnightly cycles of similar magnitude (Type  
214 1), or as a dominant signal with noticeable variability in the magnitudes of consecutive fortnightly cycles, due to a subordinate  
215 perigean-apogean influence (Type 2). Conversely, in semidiurnal areas of the world's oceans where the amplitude ratio of  $\frac{N_2}{S_2} > 1$ ,  
216 then perigean-apogean cycles will be visible, either as singularly evident monthly cycles (Type 4), or as a dominant  
217 influence with subordinate spring-neap signals (Type 3). Determining the actual boundaries between monthly tidal envelope  
218 Types 1 versus 2, and Types 3 versus 4 at a local scale involves analysis of observational records, taking into account the  
219 important influence of the  $M_2$  amplitude compared to that of the  $S_2$  and  $N_2$  amplitudes.

220 Figure 1b illustrates the division of the semidiurnal areas of the world's oceans into those where spring-neap cycles are the  
221 main monthly tidal envelope influence versus those where the perigean-apogean signal is stronger, while Fig. 1c illustrates  
222 areas of the world's oceans where spring-neap signals are very weak compared to 'perigean-apogean' influences in the monthly  
223 tidal envelope. The predictable tidal water level fluctuations such as those in our perigean-apogean monthly envelope classes  
224 are an important influence in coastal inundation hazards in different locations around the world (e.g. Wood 1978, 1986;  
225 Stephens 2015).

226 Our simple approach to classifying  $E$ , monthly tidal envelope types in semidiurnal regions, complements the existing,  
227 commonly used way of describing daily tidal forms,  $F$ , based on the amplitudes of the key diurnal ( $K_1$ ,  $O_1$ ) and semidiurnal  
228 ( $M_2$ ,  $S_2$ ) constituents. We hope that our work inspires other efforts to study tidal height variations at timescales greater than  
229 daily, work which could draw renewed attention to the fundamental role of tidal water levels in shaping coastal environments,  
230 including in hazards such as coastal flooding.

## 231 **Data Availability**

232 The tidal data used in this paper are available from LINZ (2017a; 2017b), NIWA (2017) and Walters et al. (2010). Details of  
233 the FES2014 tide model database are found via <https://www.aviso.altimetry.fr/en/data/products/auxiliary-products/global-tide-fes.html> and in Carrère et al. (2016). Appendix 1 contains the data produced from analysis of these primary resources in  
234 this paper.

237 **Table A1. Monthly tidal envelope types and values of monthly ( $E$ ) and daily ( $F$ ) form factors, and data on the amplitude ( $a_i$ ) and  
 238 phase lag ( $G_i$ , relative to Greenwich) values of 5 tidal constituents' (subscript  $i$ ) harmonic constants at 27 sea level stations around  
 239 New Zealand.**

Station name (record used)	Envelope type	$E$ value	$F$ value	M <sub>2</sub>		S <sub>2</sub>		N <sub>2</sub>		K <sub>1</sub>		O <sub>1</sub>	
				$a_i$ (cm)	$G_i$ (deg.)								
Kapiti (2011)	1	0.790	0.05	55	280	26	336	9	277	2	195	2	18
Nelson (2015)	2	0.902	0.04	133	276	40	329	23	254	6	187	1	80
Manukau (2011)	2	0.935	0.05	109	297	29	332	20	287	6	17	1	287
Taranaki (2016)	2	0.941	0.05	119	278	33	319	24	257	6	192	2	90
Onehunga (2016)	2	0.945	0.05	131	304	34	359	25	288	6	205	2	118
Westport (2015)	2	0.958	0.04	113	309	29	348	23	287	2	198	3	40
Charleston (2015/2016)	2	0.962	0.05	106	319	27	344	22	304	3	6	3	243
Puysegur Point (2012)	2	0.979	0.07	78	350	19	13	17	335	3	316	4	245
North Cape (2010)	3	1.011	0.11	80	230	15	279	16	209	8	10	2	351
Boat Cove, Rauol Island (2012)	3	1.017	0.14	50	208	9	287	10	176	5	43	3	44
Dog Island (2011)	3	1.028	0.06	91	33	18	57	21	6	2	119	4	60
Auckland (2011)	3	1.039	0.07	112	216	17	275	22	192	7	356	2	324
Bluff (2016)	3	1.040	0.05	84	48	15	75	19	23	2	133	3	71
Fishing Rock, Raoul Island (2011)	3	1.050	0.12	52	206	8	283	11	178	5	35	2	41
Lottin Point (2011)	3	1.063	0.1	70	195	9	262	14	168	6	352	2	328
Tauranga (2011)	3	1.063	0.08	70	211	9	277	14	186	5	0	1	330
Korotiti Bay (2011)	3	1.056	0.08	78	207	11	265	16	181	6	349	1	317
Moturiki (2011)	3	1.060	0.07	73	189	10	265	15	156	5	173	1	136
Green Island (2011)	3	1.084	0.08	73	81	10	91	17	50	3	93	4	44
Port Chalmers (2011)	3	1.093	0.07	77	112	9	112	17	89	3	270	3	247
Sumner (2011)	3	1.133	0.09	84	136	6	151	18	109	5	273	3	245
Gisborne (2010)	3	1.130	0.07	64	176	5	251	14	148	4	336	1	275
Napier (2011)	3	1.147	0.07	64	167	4	240	14	138	3	298	2	221
Kaikoura (2011)	4	1.162	0.12	65	146	3	171	14	117	4	275	4	233
Owenga, Chatham Islands (2011)	4	1.160	0.08	48	149	2	224	10	119	2	246	2	179
Castlepoint (2011)	4	1.167	0.09	63	159	3	225	14	129	3	280	3	219
Wellington (2011)	4	1.176	0.1	49	148	2	352	11	116	2	268	3	219
Overall range	1-4	0.79- 1.176	0.04- 0.14	48-133	-	2-40	-	9-25	-	2-8	-	1-4	-

241 **Author contribution**

242 Both authors conceived of the idea behind this paper. DH produced the initial manuscript draft. D-SB analysed the tidal data  
 243 and wrote the results sections. Both authors worked on and finalised the full manuscript.

244 **Competing interests**

245 The authors declare that they have no conflict of interest.

246 **Special issue statement (will be included by Copernicus)**247 **Acknowledgements**

248 We are grateful to Land Information New Zealand (LINZ) and the National Institute of Water and Atmospheric Research  
 249 (NIWA) for supplying the tidal data used in this research. Thank you to the University of Canterbury Erskine Programme for  
 250 supporting D.-S. Byun during his time in New Zealand; to John Thyne for supplying the Fig. 2 outline map, and to Dr Derek  
 251 Goring for interesting discussions regarding tidal data sources, to Phillip Woodworth, Glen Rowe and an anonymous reviewer  
 252 for comments that helped us improve this manuscript.

253 **References**

254 Byun, D.-S. and Hart, D. E.: Predicting tidal heights for new locations using 25h of in situ sea level observations plus reference  
 255 site records: A complete tidal species modulation with tidal constant corrections, *J. Atmos. Ocean. Tech.*, 32, 350-371, 2015.

256 Carrère L., Lyard, F., Cancet, M., Guillot, A. and Picot, N.: FES 2014, a new tidal model - validation results and perspectives  
 257 for improvements, Presentation to ESA Living Planet Conference, Prague, 2016.

258 Cartwright, D. E.: *Tides: A scientific history*, Cambridge; Cambridge University Press, 1999.

259 Courtier, A.: *Marées. Service Hydrographique de la Marine*, Paris (English translation available from:  
 260 <https://journals.lib.unb.ca/index.php/ihr/article/download/27428/1882520184>), 1938.

261 Defant, A.: *Ebb and flow: the tides of earth, air, and water*, Ann Arbor, University of Michigan Press, 1958.

262 Hart D. E., Byun D.-S., Giovinazzi S., Hughes M. W. and Gomez C.: Relative Sea Level Changes on a Seismically Active  
 263 Urban Coast: Observations from Laboratory Christchurch, Auckland, New Zealand, *Proceedings of the Australasian Coasts  
 264 and Ports Conference 2015*, 15-18 Sep 2015, 6 pp., 2015.

265 Heath, R. A.: Phase distribution of tidal constituents around New Zealand, *New Zeal. J. Mar. Fresh.*, 11(2), 383-392, 1977.

266 Heath, R. A.: A review of the physical oceanography of the seas around New Zealand—1982, *New Zeal. J. Mar. Fresh.*, 19(1),  
267 79-124, 1985.

268 LINZ, Land Information New Zealand: Sea level data downloads, <http://www.linz.govt.nz/sea/tides/sea-level-data/sea-level-data-downloads>, last access 2017a.

270 LINZ, Land Information New Zealand: Tides around New Zealand, <https://www.linz.govt.nz/sea/tides/introduction-tides/tides-around-new-zealand>, last access 2017b.

272 Masselink, G., Hughes, M., and Knight, J.: *Introduction to Coastal Processes and Geomorphology* (2 edn), Routledge, 432 pp.,  
273 2014.

274 Menéndez, M., and Woodworth, P. L.: Changes in extreme high water levels based on a quasi-global tide-gauge data set, *J. Geophys. Res.*, 115(C10) doi:10.1029/2009JC005997, 2010.

276 Nicholls, R. J., Wong, P. P., Burkett, V. R., Codignotto, J., Hay, J., McLean, R., Ragoonaden, S., Woodroffe, C. D., Abuodha,  
277 P. A. O., Arblaster, J. and Brown, B.: Coastal systems and low-lying areas, in: Parry, M. L., Canziani, O. F., Palutikof, J. P.,  
278 van der Linden, P. J. and Hanson, C. E. (ed) *Climate change 2007: impacts, adaptation and vulnerability*, Contribution of  
279 Working Group II to the fourth assessment report of the Intergovernmental Panel on Climate Change, Cambridge, UK,  
280 Cambridge University Press, 315-356, 2007.

281 NIWA, National Institute of Water and Atmospheric Research: Sea level gauge records (hourly interval),  
282 <https://www.niwa.co.nz/our-services/online-services/sea-levels>, last access 2017.

283 Olson, D.-W.: Perigean spring tides and apogean neap tides in history, *American Astronomical Society Meeting Abstracts*,  
284 219, 115.03, 2012.

285 Pawlowicz, R., Beardsley, B., and Lentz, S.: Classical tidal harmonic analysis including error estimates in MATLAB using  
286 T\_TIDE, *Comput. Geosci.*, 28(8), 929-937, doi:10.1016/S0098-3004(02)00013-4, 2002.

287 Pugh, D. T. and Woodworth, P. L.: *Sea-level science: Understanding tides, surges, tsunamis and mean sea-level changes*,  
288 Cambridge University Press, Cambridge, ISBN 9781107028197, 408 pp., 2014.

289 Pugh, D. T.: *Tides, surges and mean sea-level* (reprinted with corrections), Chichester, U.K.; John Wiley & Sons Ltd, 486 pp.,  
290 1996.

291 Stammer, D., Ray, R. D., Andersen, O. B., Arbic, B. K., Bosch, W., Carrère, L., Cheng, Y., Chinn, D. S., Dushaw, B. D.,  
292 Egbert, G. D. and Erofeeva, S. Y.: Accuracy assessment of global barotropic ocean tide models, *Rev. Geophys.*, 52(3), 243-  
293 282, doi:10.1002/2014RG000450, 2014.

294 Stephens, S.: The effect of sea level rise on the frequency of extreme sea levels in New Zealand, NIWA Client Report No.  
295 HAM2015-090, prepared for the Parliamentary Commissioner for the Environment PCE15201, Hamilton, 52 pp., 2015.

296 Stephens, S. A., Bell, R. G., Ramsay, D., and Goodhue, N.: High-water alerts from coinciding high astronomical tide and high  
297 mean sea level anomaly in the Pacific islands region, *J. Atmos. Ocean. Tech.*, 31(12), 2829-2843, 2014.

298 van der Stok, J. P.: *Wind and water, currents, tides and tidal streams in the East Indian Archipelago*. Batavia, 1897.

299 Walters, R. A., Gillibrand, P. A., Bell, R. G., and Lane, E. M.: A study of tides and currents in Cook Strait, New Zealand,  
300 Ocean Dynam., 60(6), 1559-1580, doi:10.1007/s10236-010-0353-8, 2010.

301 Walters, R. A., Goring, D. G., and Bell, R. G.: Ocean tides around New Zealand, New Zeal. J. Mar. Fresh., 35(3), 567-579,  
302 2001.

303 Wood, F. J.: The strategic role of perigean spring tides in nautical history and North American coastal flooding, 1635-1976,  
304 Department of Commerce, 1978.

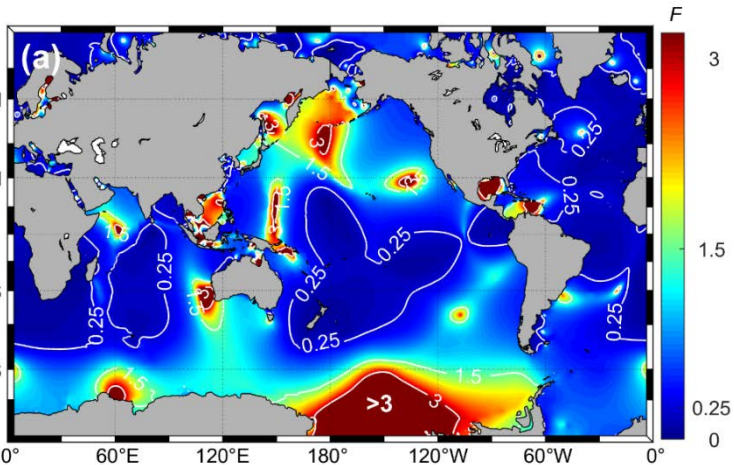
305 Wood, F. J.: Tidal dynamics: Coastal flooding and cycles of gravitational force, M.A., USA, D. Reidel Publishing Co.,  
306 Hingham, 1986.

307 Woodworth, P. L., Melet, A., Marcos, M., Ray, R. D., Wöppelmann, G., Sasak, i Y. N., Cirano, M., Hibbert, A., Huthnance, J.  
308 M., Monserrat, S., and Merrifield, M. A.: Forcing factors affecting sea level changes at the coast, Surv. Geophys., 2019.

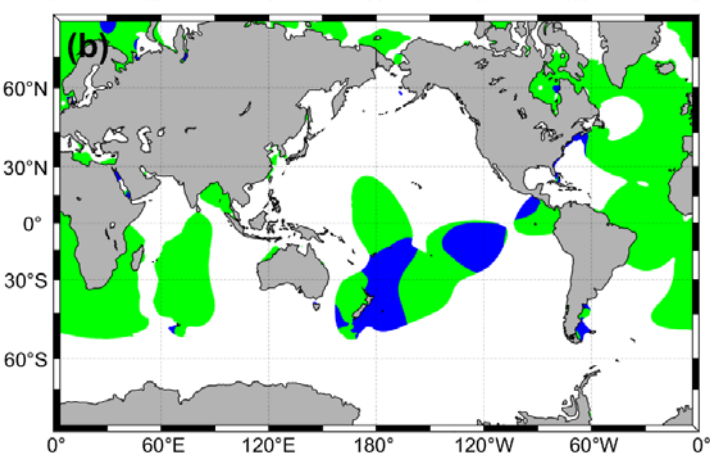
**Table 1.** Comparison of tidal constituent amplitudes, amplitude ratios (including daily tidal form factor,  $F$ , and monthly tidal envelope factor,  $E$ ) and ranges between the four distinct monthly tidal envelope types found in the 27 case study semidiurnal tide regimes of New Zealand, and compared to Equilibrium Theory amplitude ratios

Envelope type	Example sites	Amplitude (cm)						Amplitude ratio			$F$ value range, description	$E$ value range, description	
		$M_2$	$S_2$	$N_2$	$K_1$	$O_1$	$\frac{S_2}{M_2}$	$\frac{N_2}{M_2}$	$\frac{S_2}{N_2}$	$\frac{S_2+N_2}{M_2}$	$\frac{K_1}{M_2}$		
n/a	Equilibrium Theory	-	-	-	-	-	0.47	0.19	0.41	2.44	0.66	0.58	0.42
1	Kapiti	55	26	9	2	2	0.47	0.16	0.35	2.89	0.64	0.04	0.04
2	Nelson, Manukau, Taranaki, Onehunga, Westport, Charleston, Pusegar Point	78 to 133	19 to 40	17 to 25	2 to 6	1 to 4	0.24 to 0.3	0.18 to 0.22	0.58 to 0.89	1.12 to 1.74	0.45 to 0.48	0.02 to 0.06	0.01 to 0.05
3	North Cape, Boat Cove and Fishing Rock (Raoul Island), Dog Island, Auckland, Bluff, Lottin Point, Tauranga, Kororiti Bay, Moturiki, Green Island, Port Chalmers, Sumner, Gisborne, Napier	50 to 112	4 to 18	10 to 22	2 to 8	1 to 4	0.06 to 0.2	0.2 to 0.23	1.07 to 3.5	0.29 to 0.94	0.28 to 0.43	0.02 to 0.10	0.01 to 0.10
4	Kaikoura, Owenga, Castlepoint, Wellington	48 to 65	2 to 3	10 to 14	2 to 4	2 to 4	0.04 to 0.05	0.21 to 0.22	4.67 to 5.50	0.18 to 0.21	0.25 to 0.27	0.04 to 0.06	0.08 to 0.12

313

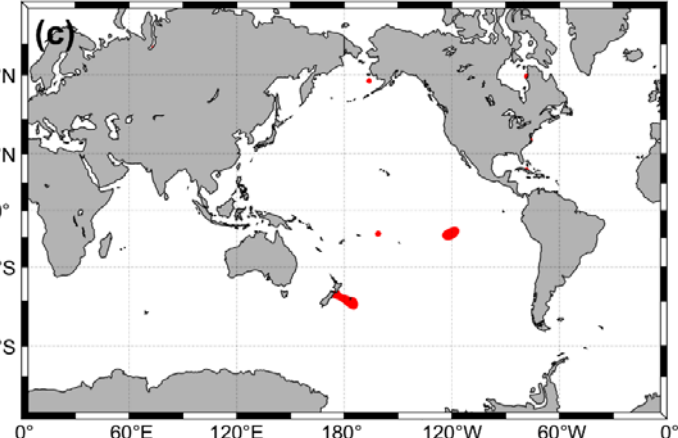


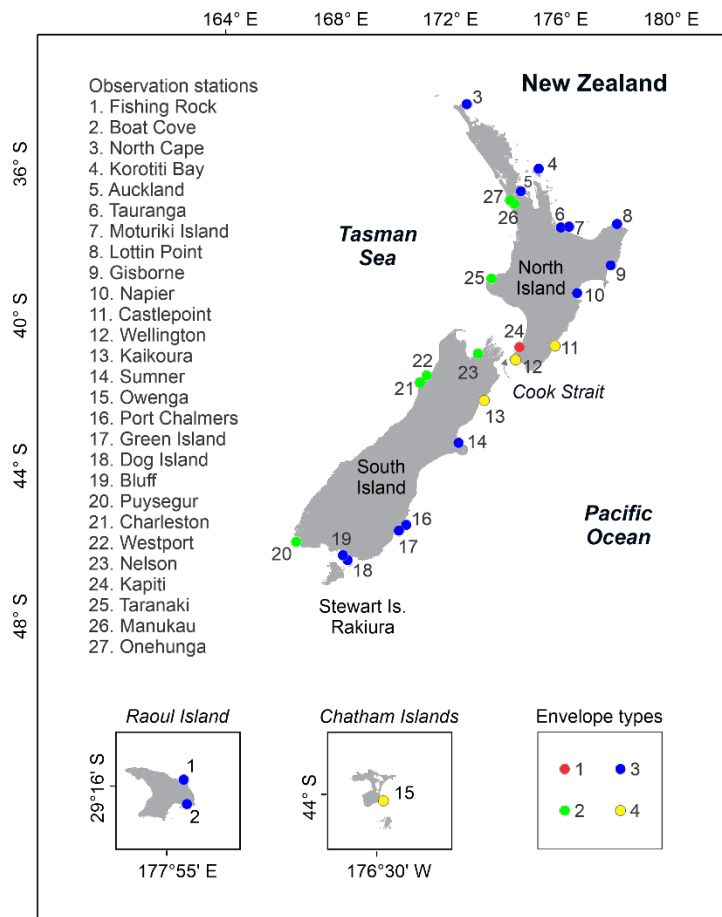
314



315

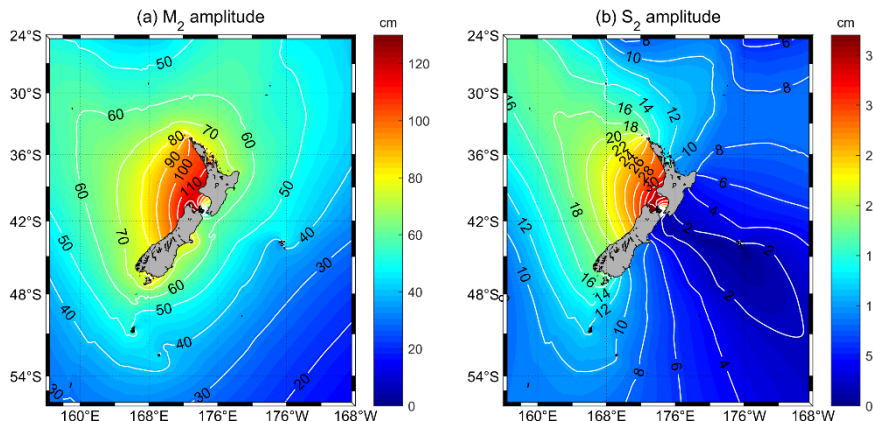
316 Figure 1. (a) Global distribution of daily form factor ( $F$ ) values, indicating daily tidal regime types ( $F < 0.25$ : semidiurnal;  $F > 0.25$  to  
 317  $F < 1.5$  mixed-mainly semidiurnal;  $F > 1.5$  to  $F < 3$ : mixed-mainly diurnal; and  $F > 3$ : diurnal, according to the classification of van der  
 318 Stok 1897, and Courtier 1938); (b) the world's semidiurnal tidal areas ( $F < 0.25$ ) divided into those where spring-neap (green) versus  
 319 perigean-apogee (blue) signals are the main influence on the monthly tidal envelope; and (c) semidiurnal tidal regimes (in red)  
 320 where the  $S_2/M_2$  constituent amplitude ratio is  $< 0.04$  and the spring-neap tidal signals are very weak as compared to perigean-  
 321 apogee signals, derived from FES2014 tidal harmonic constants.



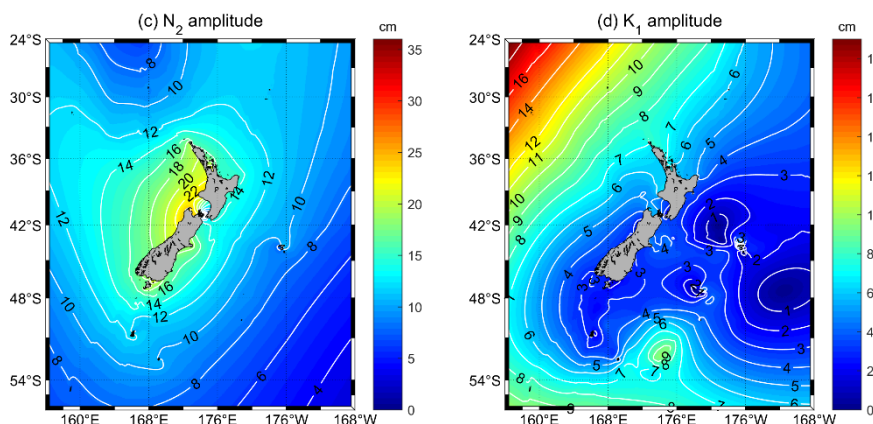


322  
323

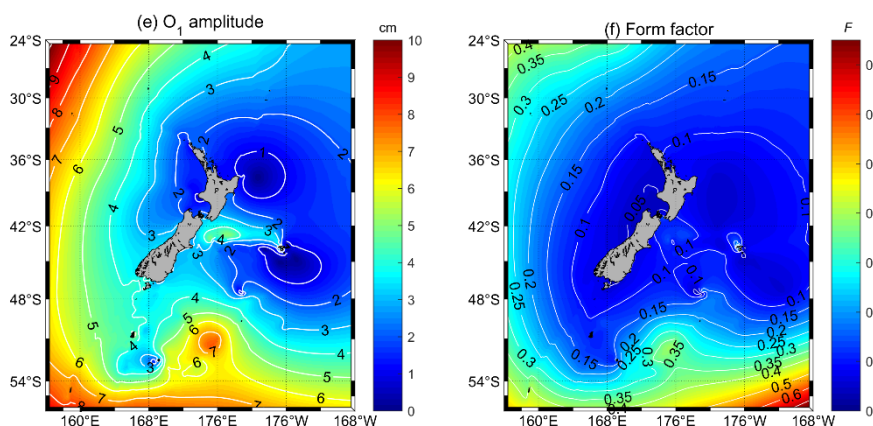
324 **Figure 2. Location of New Zealand sea level observation stations investigated in this research. Each site is coloured according to**  
325 **monthly tidal envelope type. Offshore islands are not shown to scale (Raoul and Chatham Islands).**



326



327

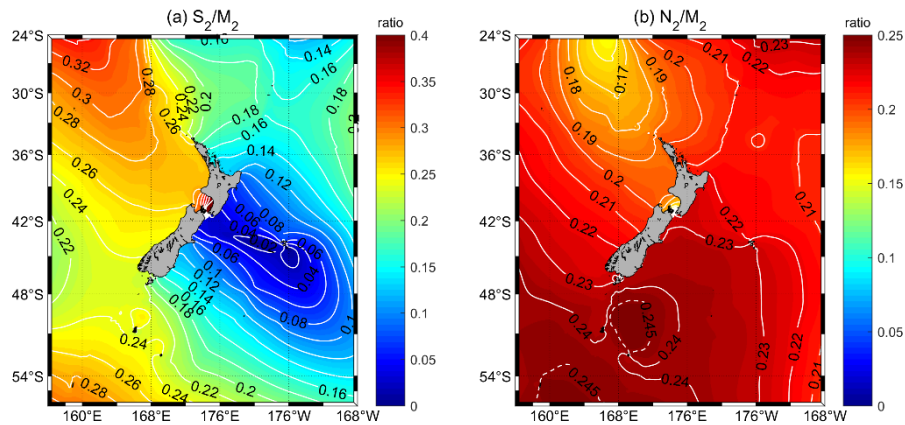


328

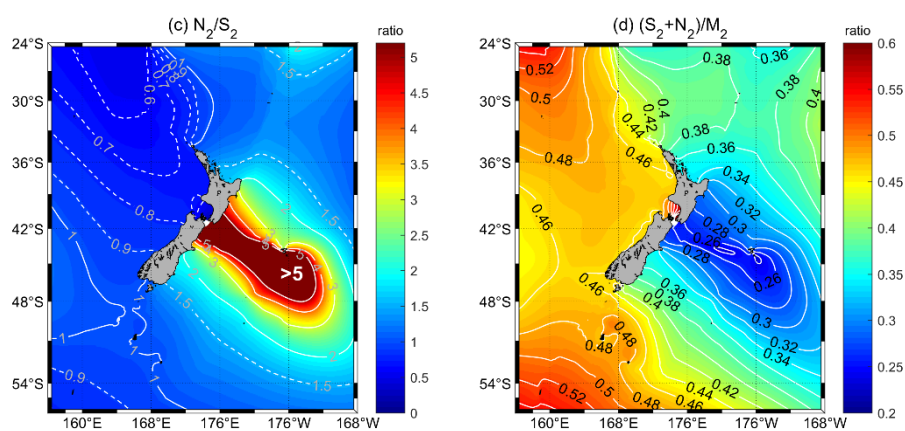
329 **Figure 3. Distribution of amplitudes for the (a) M<sub>2</sub>, (b) S<sub>2</sub>, (c) N<sub>2</sub>, (d) K<sub>1</sub>, and (e) O<sub>1</sub> tides around NZ, and (f) the resultant**

330 distribution of F, daily tidal form factor values, as calculated from the FES2014 tide model on a grid of 1°/16×1°/16. Note that the

331 amplitude colour scales vary between plots a and e.

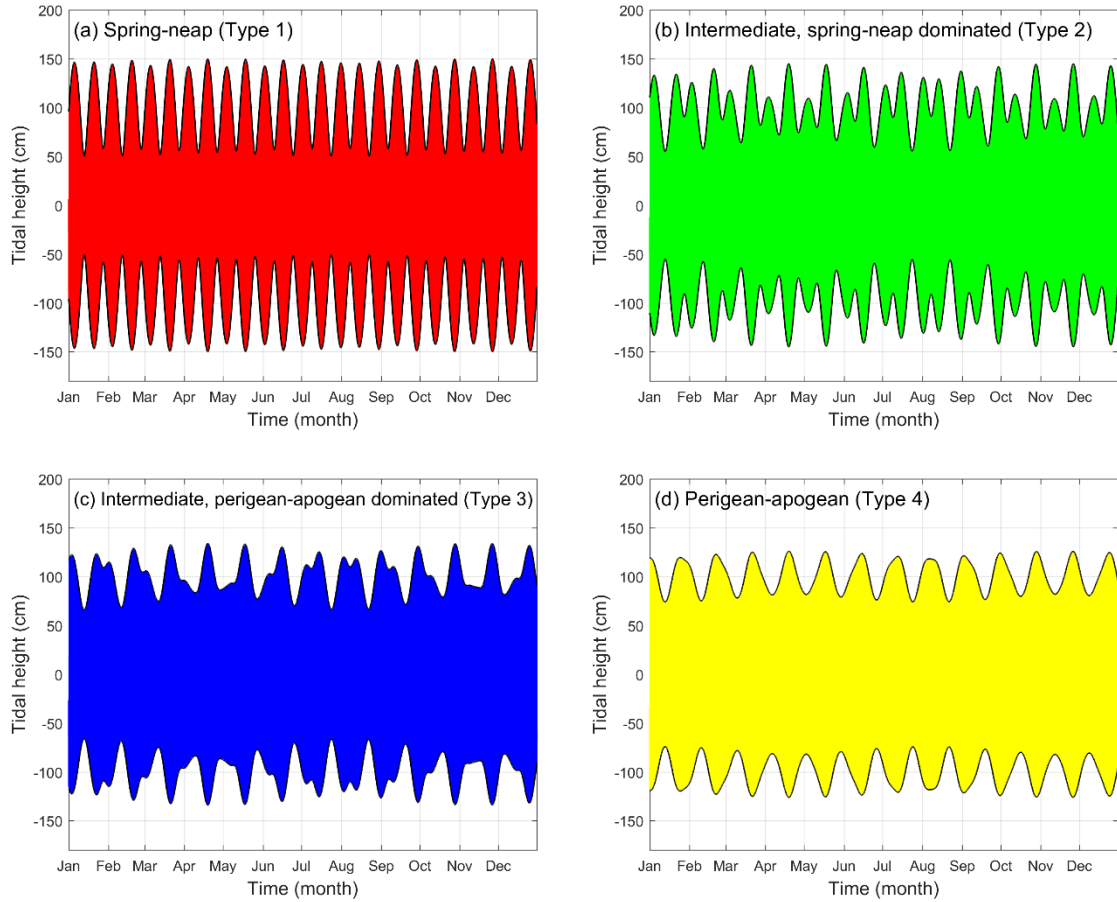


332

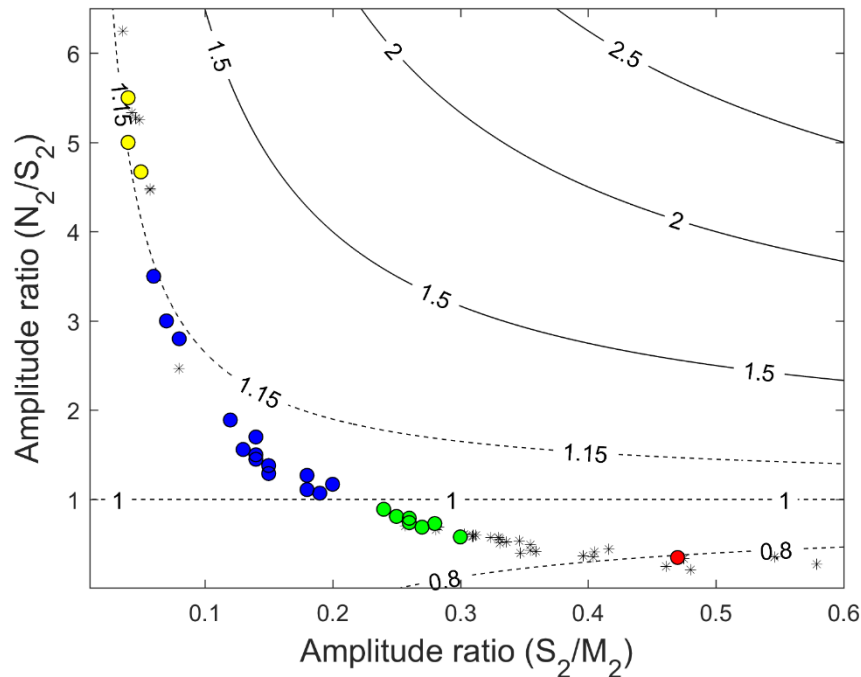


333

334 **Figure 4. Distributions of tidal constituent amplitude ratios around NZ for: (a)  $\frac{S_2}{M_2}$ ; (b)  $\frac{N_2}{M_2}$ ; (c)  $\frac{N_2}{S_2}$  and (d)  $\frac{S_2+N_2}{M_2}$ ; as calculated using**  
 335 **the FES2014 tide model on a grid of  $1^\circ/16 \times 1^\circ/16$ . Note that the amplitude colour scales vary between plots a and d.**

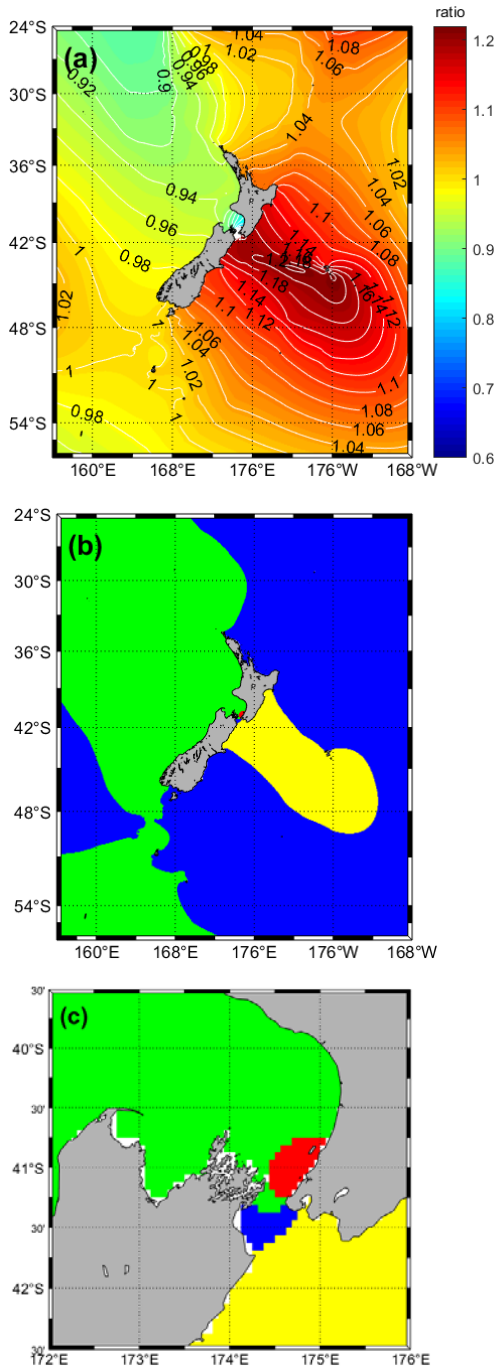


336 **Figure 5. Idealised examples of four different monthly tidal envelopes over one year, calculated using the amplitude value  $M_2 = 100$**   
 337 **cm and the amplitude ratio values of: (a)  $\frac{S_2}{M_2} = 0.46$ ,  $\frac{S_2}{N_2} = 11.5$ ,  $\frac{N_2}{M_2} = 0.04$ ; (b)  $\frac{S_2}{M_2} = 0.27$ ,  $\frac{S_2}{N_2} = 1.5$ ,  $\frac{N_2}{M_2} = 0.18$ ; (c)  $\frac{S_2}{M_2} = 0.12$ ,**  
 338  **$\frac{S_2}{N_2} = 0.54$ ,  $\frac{N_2}{M_2} = 0.22$ ; and (d)  $\frac{S_2}{M_2} = 0.04$ ,  $\frac{S_2}{N_2} = 0.18$ ,  $\frac{N_2}{M_2} = 0.22$ . Note that the  $E$  values of these plots are: (a) 0.71; (b) 0.93; (c)**  
 339 **1.09; and (d) 1.17.**



340

341 **Figure 6.** Plot of the relationship between the  $\frac{N_2}{S_2}$  and  $\frac{S_2}{M_2}$  amplitude ratios (y and x axes respectively) and  $E$  values (shown as plot  
 342 contours), with data points corresponding to New Zealand waters monthly tidal envelope Type 1 sites (red dots), Type 2 sites (green  
 343 dots), Type 3 sites (blue dots), and Type 4 sites (yellow dots), (all from Table A1); and tidal data representative of the greater Cook  
 344 Strait (black stars) from Walters et al. (2010, Tables 1 and 3).



345 **Figure 7.** (a) Distribution of monthly tidal envelope factor ( $E$ ) values; and (b) monthly tidal envelope types; in the waters around  
 346 New Zealand, including (c) in the Cook Strait area between the two main islands; all calculated using FES2014 data. In (b) and (c),  
 347 envelope type 1 areas are shown in red; type 2 in blue; type 3 in green; and type 4 in yellow. See Fig. 5 for definitions and examples  
 348 of monthly tidal envelope factor classes and patterns.